Spotlight on Molecular Profiling

Asparagine synthetase as a causal, predictive biomarker for L-asparaginase activity in ovarian cancer cells

Philip L. Lorenzi,[1] William C. Reinhold,[1] Martina Rudelius,[4] Michele Gunsior,[2] Uma Shankavaram,[1] Kimberly J. Bussey,[1] Uwe Scherf,[1] Gabriel S. Eichler,[1] Scott E. Martin,[3] Koei Chin,[6] Joe W. Gray,[6] Elise C. Kohn,[5] Ivan D. Horak,[7] Daniel D. Von Hoff,[8] Mark Raffeld,[4] Paul K. Goldsmith,[2] Natasha J. Caplen,[3] and John N. Weinstein[1]

[1]Genomics and Bioinformatics Group, Laboratory of Molecular Pharmacology, [2]Antibody and Protein Purification Unit, and [3]Gene Silencing Section, Office of Science and Technology Partnerships, Office of the Director, Center for Cancer Research, National Cancer Institute, NIH; [4]Special Diagnostics Section and [5]Molecular Signaling Section, Laboratory of Pathology, National Cancer Institute, NIH, Bethesda, Maryland; [6]Cancer Research Institute, University of California San Francisco, San Francisco, California; [7]Enzon Pharmaceuticals, Inc., Piscataway, New Jersey; and [8]Translational Genomics Research Institute, Phoenix, Arizona

Abstract

L-Asparaginase (L-ASP), a bacterial enzyme used since the 1970s to treat acute lymphoblastic leukemia, selectively starves cells that cannot synthesize sufficient asparagine for their own needs. Molecular profiling of the NCI-60 cancer cell lines using five different microarray platforms showed strong negative correlations of asparagine synthetase (ASNS) expression and DNA copy number with sensitivity to L-ASP in the leukemia and ovarian cancer cell subsets. To assess whether the ovarian relationship is causal, we used RNA interference to silence *ASNS* in three ovarian lines and observed 4- to 5-fold potentiation of sensitivity to L-ASP with two of the lines. For OVCAR-8, the line that expresses the least ASNS, the potentiation was >500-fold. Significantly, that potentiation was >700-fold in the multidrug-resistant derivative OVCAR-8/ADR, showing that the causal relationship between ASNS expression and L-ASP activity survives development of classical multidrug resistance. Tissue microarrays confirmed low ASNS expression in a subset of clinical ovarian cancers as well as other tumor types. Overall, this pharmacogenomic/pharmacoproteomic study suggests the use of L-ASP for treatment of a subset of ovarian cancers (and perhaps other tumor types), with ASNS as a biomarker for patient selection. [Mol Cancer Ther 2006;5(11):2613–23]

Introduction

The bacterial enzyme L-asparaginase (L-ASP) was screened for activity against a variety of tumor types in the 1970s, but its activity was sporadic and statistically nonsignificant in all but one cancer type, acute lymphoblastic leukemia, for which it was Food and Drug Administration approved in 1978. The rationale for selective activity of L-ASP in acute lymphoblastic leukemia is that those cells require more asparagine than they can synthesize endogenously and must therefore scavenge circulating asparagine to survive. More recent studies have suggested a link between L-ASP activity and expression levels of asparagine synthetase (ASNS), the enzyme responsible for endogenous synthesis of asparagine from aspartate (1–3). That apparent mechanism of action is particularly interesting because it differs from those of other anticancer drug classes and because the mechanism does not require the enzyme-drug to enter the tumor or even escape from the bloodstream. We wondered, in that context, whether molecular profiling data from the NCI-60 cell lines would suggest the use of ASNS as a biomarker to predict L-ASP efficacy in tumor types other than acute lymphoblastic leukemia.

The NCI-60 panel consists of 60 human cancer cell lines used by the Developmental Therapeutics Program of the U.S. National Cancer Institute (NCI) to screen >100,000 chemical compounds for anticancer activity since 1990 (4–7). Patterns of drug activity and molecular profiling of cells in the screen have yielded rich information on mechanisms of drug action and inhibition (2, 4, 8, 9). Overall, the NCI-60 panel has been characterized at the molecular level more extensively than any other set of cells,

Received 7/31/06; revised 10/4/06; accepted 10/5/06.

Grant support: The Intramural Research Program of the NIH, National Cancer Institute, Center for Cancer Research; Pharmacology Research Associate Fellowship from National Institute of General Medical Sciences, NIH (P.L. Lorenzi); and program project grant CA 109552 from the Department of Health and Human Services (D.D. Von Hoff).

The costs of publication of this article were defrayed in part by the payment of page charges. This article must therefore be hereby marked advertisement in accordance with 18 U.S.C. Section 1734 solely to indicate this fact.

Note: Competing interests statement: I.D. Horak is employed by Enzon Pharmaceuticals, Inc., which has an interest in pegylated L-ASP.

Requests for reprints: John N. Weinstein, Genomics and Bioinformatics Group, Room 5056B, 37 Convent Drive, Bethesda, MD 20892. Phone: 301-496-9571. E-mail: jw4i@nih.gov

doi:10.1158/1535-7163.MCT-06-0447

and additional characterizations appear in this issue, inaugurating *Molecular Cancer Therapeutics'* "Spotlight on Molecular Profiling" series (9a, 9b). A number of molecular data sets have been incorporated into a user-friendly web-based tool (CellMiner) for "integromic" analysis (9a) across molecular data types.[9]

When we previously looked for a correlation between *ASNS* mRNA expression and L-ASP activity, data derived from cDNA expression microarrays showed a statistically significant but only moderately large negative correlation (−0.44; bootstrap 95% confidence interval, −0.58 to −0.25) across the 60 cell lines (2). However, the leukemia subpanel showed a remarkable negative correlation (−0.98; −1.00 to −0.93). More interestingly, the ovarian subpanel also showed a negative correlation (−0.89; −0.98 to −0.41), which seemed to be statistically significant but did not survive correction for multiple comparisons. However, our subsequent array comparative genomic hybridization (CGH) data revealed a strong negative correlation (−0.98; −1.00 to −0.84) between L-ASP activity and DNA copy number near the *ASNS* locus on 7q, and that observation did survive correction for multiple comparisons (10).

Given the uncertainties of microarray expression analysis, however, we wanted to show the correlation using additional methods. Accordingly, we have now extended the study to three additional platforms for measurement of mRNA expression (Affymetrix Hu6800, U95, and U133 chips). The L-ASP/ASNS relationship holds up across all of those platforms. To test whether the L-ASP/ASNS relationship is causal, we used RNA interference (RNAi) and an optimized assay for L-ASP cytotoxicity in three ovarian cancer cell lines that exhibit a range of ASNS expression levels. We report here, using assays at both mRNA and protein levels, that L-ASP cytotoxicity is causally and functionally linked to ASNS expression. Overall, the studies described here suggest the possible use of L-ASP for treatment of subsets of ovarian cancers (and possibly other cancer types), with ASNS as a biomarker for patient selection. Toward that end, we have opened a phase I clinical trial in patients with solid tumors and non-Hodgkin's lymphoma at three academic institutions, with ASNS assessed retrospectively as a biomarker.

Materials and Methods

Transcript Expression Profiling and Array CGH

ASNS transcript expression levels were obtained from four different NCI-60 data sets, two of them previously published. *ASNS* data from the other two are presented here for the first time. The first two were based on 9,706-clone spotted cDNA arrays (2, 11) and ~6,800 probe set 25-mer Affymetrix oligonucleotide arrays (12). The unpublished data[9] were from the five-chip (~60,000 probe set) HG-U95 Affymetrix array set and the two-chip (~45,000 probe set) HG-U133 Affymetrix array in studies done with GeneLogic, Inc. (Gaithersburg, MD). The protocol for cell harvests was as follows. Seed cultures of the 60 cell lines were drawn from aliquoted stocks, passaged once in T-162 flasks and monitored frequently for degree of confluence. The medium was RPMI 1640 with phenol red, 2 mmol/L glutamine, and 5% fetal bovine serum. For compatibility with our other profiling studies, all fetal bovine sera were obtained from the same large batches as were used by the Developmental Therapeutics Program. One day before harvest, the cells were refed. Attached cells were harvested at ~80% confluence, as assessed for each flask by phase microscopy. Suspended cells were harvested at ~0.5×10^6/mL. In pilot studies, samples of medium showed no appreciable change in pH between refeeding and harvest, and no color change in the medium was seen in any of the flasks harvested. The time from incubator to stabilization of the preparation was kept to <1 minute. Total RNA was purified using the Qiagen (Valencia, CA) RNeasy Midi Kit according to the instructions of the manufacturer. The RNA was then quantitated spectrophotometrically and aliquoted for storage at −80°C. The samples for HG-U95 and HG-U133 microarrays were labeled and hybridized to the arrays according to standard procedures by GeneLogic.[10] Our protocols for labeling and hybridization to cDNA microarrays (2, 11) in a collaboration with the Brown/Botstein laboratory and hybridization to Affymetrix HU6800 arrays (12) in a collaboration with the Lander/Golub laboratory have previously been described. Likewise, our procedures for purification of DNA and its use in array CGH with ''OncoBAC'' DNA microarrays in a collaboration with the laboratory of Joe Gray have been described and the data presented elsewhere (10).

Cell Culture and RNA Interference

Cell lines were routinely maintained in RPMI 1640 containing 5% fetal bovine serum and 2 mmol/L L-glutamine. For mRNA and 3-(4,5-dimethyl-thiazol-2yl)-5-(3-carboxymethoxyphenyl)-2-(4-sulfophenyl)-2*H*-tetrazolium (MTS) assays, transfections mediated by cationic lipid were done in 96-well plates. Cells were seeded on a complex of the appropriate siRNA (Qiagen, Inc., Germantown, MD) and Oligofectamine (Invitrogen, Carlsbad, CA) in unsupplemented growth medium. Final amounts in each well were 50 nmol/L siRNA, 0.475 μL Oligofectamine, and 5,000 OVCAR-4 cells in 100 μL medium; 30 nmol/L siRNA, 0.40 μL Oligofectamine, and 4,300 OVCAR-3 cells in 100 μL medium; 5 nmol/L siRNA, 0.75 μL Oligofectamine, and 2,750 OVCAR-8 cells in 100 μL medium; and 5 nmol/L siRNA, 0.75 μL Oligofectamine, and 4,700 OVCAR-8/ADR cells in 100 μL medium. Three replicate wells were used in mRNA determinations. The amount of Oligofectamine was scaled to 200,000 cells per well in six-well plates for duplicate protein determinations. The ASNS target sequences of the synthetic siRNAs were designed against NM_001673 but recognize all three ASNS transcript variants. The siASNS.1 sequence consisted of sense

[9] http://discover.nci.nih.gov; Shankavaram et al., *Mol Cancer Ther,* submitted.

[10] http://www.genelogic.com/docs/pdfs/dataGenProductSheet.pdf.

r(GGAUACUGCCAAUAAGAAA)dTdT and antisense r(UUUCUUAUUGGCAGUAUCC)dAdG, designed against the target CTGGATACTGCCAATAAGAAA (exon 5, nucleotide 556). The siASNS.2 sequence consisted of sense r(GAAGCUAAAGGUCUUGUUA)dTdT and antisense r(UAACAAGACCUUUAGCUUC)dTdG, designed against the target CAGAAGCTAAAGGTCTTGTTA (exon 5/6, nucleotide 658). The negative control (siNeg) sequence consisted of r(UUCUCCGAACGUGUCACGU)dTdT and r(ACGUGACACGUUCGGAGAA)dTdT strands (Qiagen, Germantown MD). Cells and complex were incubated for 1 hour at room temperature before transferring to an incubator.

Detection of *ASNS* mRNA

ASNS mRNA levels were assayed at 48 hours using the Quantigene Branched-DNA Assay (probe set nucleotides 670–1,321, which recognizes all three *ASNS* transcript variants) according to the protocol of the manufacturer (Genospectra, Inc., Fremont, CA). The luminescence of each sample was measured with a Perkin-Elmer Victor3 V 1420 Multilabel Counter. Each background signal value (absence of capture probe) was subtracted from the corresponding *ASNS* or *cyclophillin-B* (*PPIB*; probe set nucleotides 74–432) value to correct for nonspecific binding. *ASNS* levels for a given sample were then normalized to *PPIB* levels for that sample. Normalized *ASNS* levels in siASNS-transfected cells were compared with those in siNeg-transfected cells, which served as the control.

Detection of ASNS Protein

At selected time points, cells seeded in six-well plates for protein determination were washed twice with ice-cold PBS. Ice-cold lysis buffer [20 mmol/L Tris (pH 8), 137 mmol/L NaCl, 1 mmol/L $MgCl_2$, 1 mmol/L $CaCl_2$, 1% Triton X-100, 10% glycerol, 1 mmol/L phenylmethylsulfonyl fluoride] was then added to each well and plates were rocked for 5 minutes at 4°C. The lysate was centrifuged at 14,000 rpm for 10 minutes, and the supernatant was then assayed for total protein using the Bio-Rad DC Protein Assay (Bio-Rad Laboratories, Hercules, CA) and a bovine serum albumin standard.

For Western blots, 10 μg of supernatant were loaded onto 10% acrylamide gels, with the exception that 5 μg were loaded for all OVCAR-3 samples. After electrophoresis and transfer to polyvinylidene difluoride membranes, nonspecific binding was minimized by blocking for 2 hours with TBST containing 1% (w/v) polyvinylpyrrolidone and 10% (w/v) dextran (Sigma-Aldrich, St. Louis, MO) at room temperature. The primary antibody, rabbit anti-human ASNS, was added directly to the blocking solution at 0.4 μg/mL. IRDye 800 goat anti-rabbit secondary antibody (Rockland, Gilbertsville, PA) was prepared at 1:6,000 in fresh blocking solution. Membranes were incubated with primary antibody for 2 hours and subsequently with secondary antibody for 4 hours with gentle rocking at room temperature. The membranes were washed four times with TBST between steps. Membranes were scanned on a Li-Cor Odyssey Imager. The signal was related linearly to the amount of lysate up to at least 10 μg of total protein (data not shown). To confirm specificity of the primary antibody, we treated a replicate membrane with nonspecific rabbit immunoglobulin G instead of primary antibody. It yielded no bands (data not shown). Bands were quantitated using the Odyssey version 1.2 software. Relative ASNS levels for the three ovarian cell lines (Fig. 2B) were determined by normalizing the ASNS intensity for siNeg-treated 24-, 48-, 72-, and 96-hour samples to the total amount of protein loaded and then averaging those normalized values. After quantitation and plotting of the data in Fig. 2C, the ''Autolevels'' (Shft+Ctrl+L) function in Adobe Photoshop was used to enhance contrast so that the bands would show up well in the printed figures. Because the enhancement was done on the entire gel image for a given experiment, the adjustment did not appreciably affect relative intensities.

Background was generally negligible but was nevertheless accounted for by the Li-Cor Odyssey software. Samples inoculated with the nonspecific siNeg sequence served as control. Protein levels obtained for siASNS-treated cells were divided by the corresponding levels for siNeg-treated cells and multiplied by 100 to yield percent control. Percent control values were then averaged and SDs computed ($n = 3$ for mRNA; $n = 2$ for protein).

MTS Proliferation Assay

L-ASP activity was determined by measuring formazan production from MTS (Promega, Madison, WI), with drug concentrations tested in triplicate in each experiment. Serial dilutions of *E. coli* asparaginase (stock 500 units/mL in molecular biology grade H_2O; Sigma, St. Louis, MO) were prepared in medium at room temperature. At 48 hours after seeding, cells were washed by aspiration of the supernatant and 150 μL of drug-containing medium were added. Another 48 hours later, the drug solution was aspirated and 120 μL of MTS-containing medium were added according to the protocol of the manufacturer (Promega). The plates were incubated at 37°C and read at 490 nm between 1 and 4 hours. Using GraphPad Prism 4.02 (GraphPad Software, Inc., San Diego, CA), we log transformed the drug concentrations and did nonlinear regression on the A_{490} data using the sigmoidal dose response model with variable slope. Mean EC_{50} values, SEs, and 95% confidence intervals were determined from the logistic fits.

Cell Pellet Immunohistochemistry

Cultured ovarian cells were harvested and clotted with thrombin (thrombin, Topical USP). After fixation in 10% formalin, cells were embedded in paraffin and 5-μm sections were cut. Deparaffinized slides were placed in 10 mmol/L citrate buffer (pH 6.0) containing 0.1% Tween 20, and heat-induced antigen retrieval was done using a microwavable pressure cooker (Nordicware, Minneapolis, MN) under maximum heat and pressure for 20 minutes. Following antigen retrieval, the slides were incubated with an affinity-purified rabbit polyclonal antibody produced against ASNS (1:3,000).[11] Signal was detected using an

[11] Gunsior et al., in preparation.

automated immunostainer (DakoCytomation, Carpinteria, CA) and a horseradish peroxidase/3,3′-diaminobenzidine polymer–based rabbit antibody detection system (Envision+, DakoCytomation) according to the recommendations of the manufacturer. Images were visualized under an Olympus BX41 microscope equipped with an Olympus UPlan Fl 20×/0.5 (8/0.17), captured with an Olympus DP12 digital camera, and processed with Photoshop 6.0 software (Adobe Systems, San Jose, CA).

Tissue Array Immunohistochemistry

TARP5-T-BO-1, T-CL-1, and MTA-5 tumor tissue microarrays, produced as previously described (13), were obtained from the NCI Tissue Array Research Program (TARP; Frederick, MD). Sections (5 μm) were cut from the array blocks using tape sectioning materials from Instrumedics (Hackensack, NJ). Immunohistochemical staining was done as described for the cell blocks, with the exception that two antibody dilutions were used (1:1,500 and 1:3,000). Staining intensity was graded on an arbitrary four-point scale: 0, no staining; 1+, faint or weak staining; 2+, moderate staining; and 3+, strong staining. Only intact cores containing tumor cells were scored. The TARP5-T-BO-1 array contained 54 scoreable ovarian cancers and 35 scoreable breast cancers. The T-CL-1 array contained 63 scoreable colon cancers and 77 scoreable lung cancers. The MTA-5 array contained 46 scoreable prostate cancers, 22 scoreable lymphomas, and 11 scoreable head and neck tumors. The tissue microarray from Cybrdi, Inc. included 69 ovarian cancers and 3 normal ovarian samples (all scoreable) and the array from US BioMax, Inc. (Ijamsville, MD) contained 173 primary ovarian cancers (172 scoreable) and 8 normal ovarian samples. Tissue microrrays were scanned with an Epson perfection 4800 scanner; individual core images were visualized as described for cell blocks.

Results

ASNS Expression and DNA Copy Number Are Negatively Correlated with L-ASP Activity

ASNS expression was evaluated in all seven of the NCI-60 ovarian cell lines using four different microarray platforms: cDNA (2), Affymetrix Hu6800 (12), Affymetrix U95, and Affymetrix U133 arrays.[9] For the relationship between ASNS expression and L-ASP-activity, those platforms yielded Pearson correlation coefficients and 95% confidence intervals of −0.89 (−0.98 to −0.41), −0.90 (−0.98 to −0.46), −0.85 (−0.98 to −0.28), and −0.86 (−0.98 to −0.28), respectively (Fig. 1). The data from U95 and U133 arrays have not previously been reported. CGH using bacterial artificial chromosome microarrays (10) yielded a correlation coefficient of −0.98 (−1.00 to −0.84) for the relationship between *ASNS* DNA copy number (relative to mean ploidy) and L-ASP activity in the ovarian lines. To assess ASNS/L-ASP correlations in relation to the genome-wide distribution of correlations for each data set, we calculated the correlation of L-ASP activity with expression of each gene for each microarray platform. The ASNS/L-ASP correlation was ranked in the top 1.9, 0.3, 2.4, 1.6, and 0.4 percentiles for the cDNA, Hu6800, U95, U133, and aCGH platforms, respectively. Notably, the ASNS/L-ASP correlation was the strongest of all 269 measured correlations in the CGH data set.

ASNS mRNA Is Silenced by Synthetic siRNAs Targeted to *ASNS*

Two synthetic small interfering RNAs (siASNS.1 and siASNS.2) targeted to *ASNS* were transfected into OVCAR-3, OVCAR-4, and OVCAR-8 cells. Consistent with the microarray data (Fig. 1), a branched-DNA assay for mRNA expression indicated that OVCAR-3 and OVCAR-4 express ~3.0 and 3.5 as much *ASNS* mRNA as do OVCAR-8 cells (Fig. 2A). Forty-eight hours after transfection of siASNS.1 or siASNS.2, *ASNS* mRNA levels were reduced by 83% or 79%, respectively, in OVCAR-4 cells (relative to the levels in siNeg-transfected controls). The corresponding reductions were 81% or 76% for OVCAR-3 and 87% or 80% for OVCAR-8.

ASNS Protein Expression Is Silenced by siRNA Targeted to *ASNS*

From a functional perspective, we are more interested in protein expression than in transcript expression, and one may not reflect the other (14, 15). Accordingly, we analyzed the time course of ASNS protein knockdown following RNAi. Lysates prepared from siRNA-transfected OVCAR-3, OVCAR-4, and OVCAR-8 cells were Western blotted using a polyclonal rabbit anti-human ASNS antibody[11] for detection and quantitation. OVCAR-3, OVCAR-4, and OVCAR-8 cells exhibited medium, high, and low protein levels, respectively, when transfected with siNeg (Fig. 2B). The two siRNAs targeted against *ASNS* yielded similar magnitudes and durations (4–5 days) of ASNS silencing (Fig. 2C). The 4- to 5-day period provided a window of time for pharmacologic experiments. ASNS protein was assessed over 8 days in the OVCAR-8 cell line to confirm that the transfection was transient; protein levels had returned to near-control levels by day 8.

L-ASP Cytotoxicity Is Potentiated by siRNAs Targeted to *ASNS*

To answer our central question about the nature of the correlation between ASNS expression and L-ASP activity, we silenced *ASNS* in the three ovarian cell lines, administered L-ASP 2 days later, and measured L-ASP activity with an MTS-based cytotoxicity assay after 2 or 3 days of exposure to the enzyme. The baseline sensitivities of the three lines to L-ASP in the MTS assay (as assessed in siNeg-transfected cells) were consistent with previous results obtained using a sulforhodamine B assay in the NCI-60 screen (2, 16); OVCAR-4 showed the greatest resistance to L-ASP, and OVCAR-8 the greatest sensitivity (Fig. 3A; Supplementary Table S1[12]). Transfection of OVCAR-4 cells with siASNS yielded 4.1- to 4.9-fold potentiation of L-ASP activity, suggesting that *ASNS* RNAi can affect drug response even in the presence of relatively high ASNS

[12] Supplementary material for this article is available at Molecular Cancer Therapeutics Online (http://mct.aacrjournals.org/).

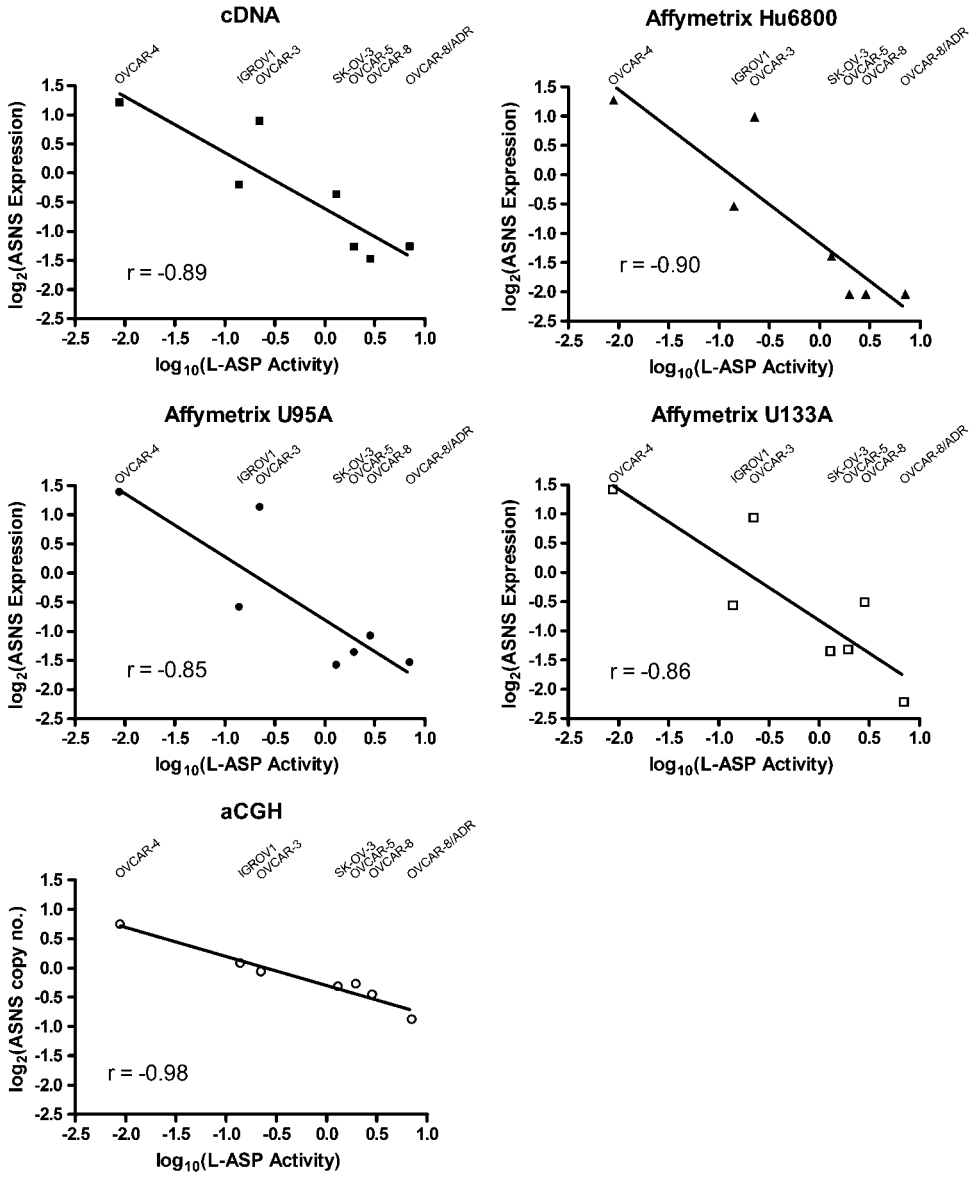

Figure 1. Correlation of L-ASP activity with *ASNS* expression and *ASNS* DNA copy number. *ASNS* transcript levels were measured using four different microarray platforms: cDNA array, Affymetrix Hu6800 array, Affymetrix U95 array, and Affymetrix U133 array. *ASNS* copy number (relative to mean ploidy) was assessed from array CGH, based on a BAC probe on 7q near the locus of *ASNS*.

levels. OVCAR-3 cells, which express slightly less ASNS, yielded a similar degree of L-ASP potentiation, 3.2- to 4.3-fold. The potentiation in both OVCAR-4 and OVCAR-3 was, thus, roughly proportional to the observed degree of *ASNS* silencing, 4- to 5-fold. The low-ASNS OVCAR-8 cells, on the other hand, yielded a surprise: L-ASP was potentiated >500-fold, an extent far greater than the ~5-fold *ASNS* silencing. That potentiation was highly reproducible; a second, independent experiment yielded 560- and 550-fold potentiation with siASNS.1 and siASNS.2, respectively (data not shown). Those RNAi studies answered our central question by showing a causal link between ASNS expression and sensitivity to L-ASP in ovarian cancer cell lines. The link was clear-cut over a wide range of ASNS expression, but it was most striking for the cell line with lowest baseline expression. Statistics of the pharmacologic assays can be found in Supplementary Table S1.

Reconstitution of ASNS Expression Abrogates L-ASP Potentiation

To test for reversibility of the potentiation, we assayed L-ASP activity after ASNS protein had returned to near-baseline levels 8 days after siASNS transfection. The cells were exposed to L-ASP for 2 days starting on day 8. The MTS assay on day 10 (Fig. 3B) indicated that the previously observed 500-fold potentiation had been abolished on reconstitution of ASNS expression.

L-ASP Activity Is Potentiated by siRNA Targeted to *ASNS* in a Multidrug-Resistant Cell Line

Because the majority of ovarian cancer patients develop resistance to chemotherapeutics, we asked whether the ASNS/L-ASP relationship would be maintained after the development of classical multidrug resistance. To answer that question, we used OVCAR-8/ADR, a derivative of OVCAR-8 grown under selective pressure for resistance

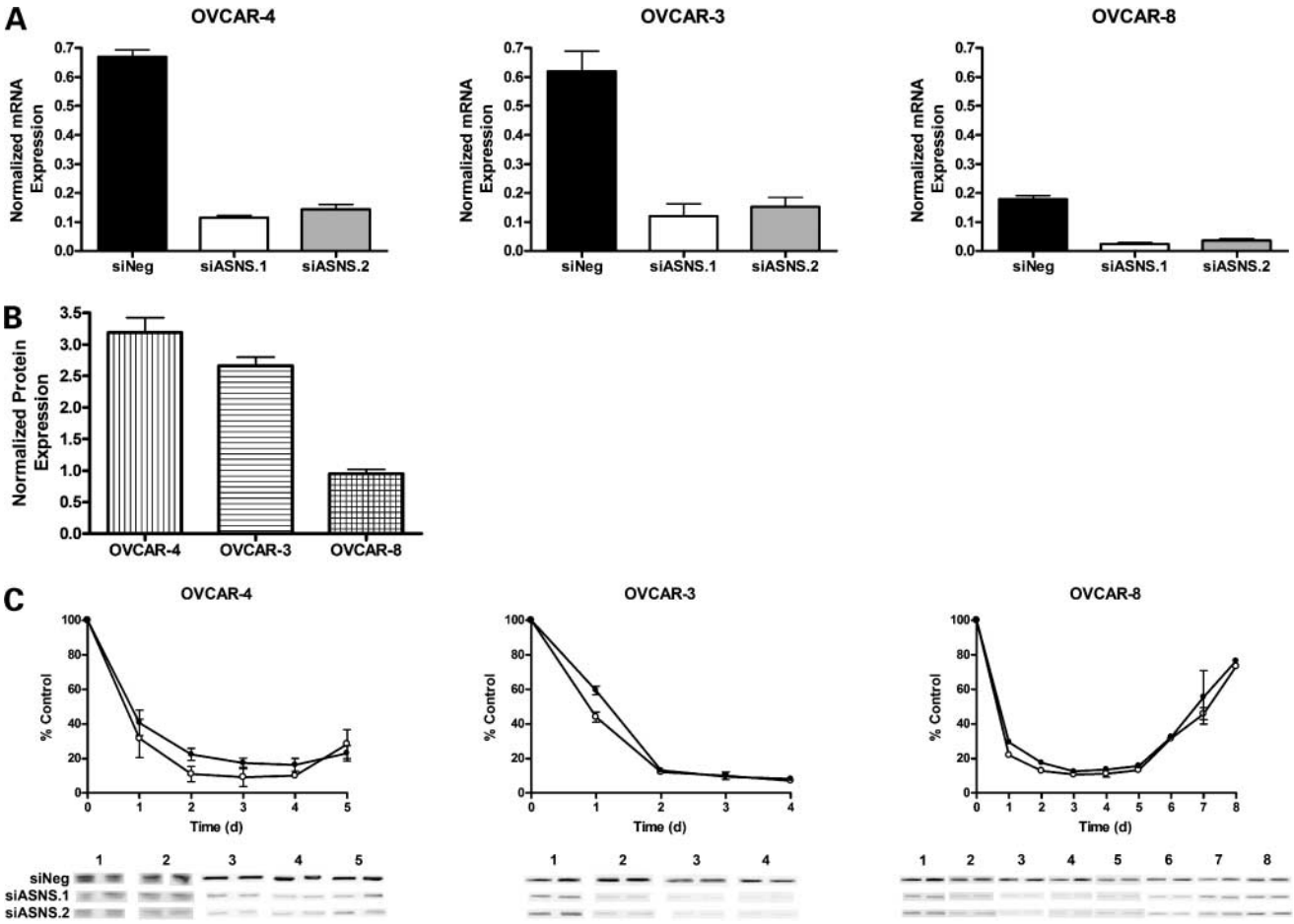

Figure 2. ASNS expression following synthetic siRNA transfection of ovarian cancer cell lines. **A,** branched-DNA assay for *ASNS* mRNA 48 h after transfection of siNeg, siASNS.1, or siASNS.2. *ASNS* levels for a given sample were normalized to *PPIB* levels for that sample. **B,** quantitation of ASNS protein from Western blots. Protein levels represent means of replicate cultures treated for 24, 48, 72, or 96 h with siNeg and normalized by total protein loaded on the gel. **C,** time course of protein expression quantitated from Western blots after transfection of siASNS.1 (○) or siASNS.2 (●), expressed as percent of the corresponding siNeg control level.

to Adriamycin (doxorubicin) and previously shown to exhibit a multidrug resistant phenotype (17, 18). [OVCAR-8/ADR was originally designated as MCF7/ADR and later as NCI/ADR because of uncertainty about its lineage, but we found by CGH and spectral karyotyping (10, 19) that it is actually a derivative of OVCAR-8.] We first noted that *ASNS* expression in OVCAR-8/ADR was approximately the same as in the parental OVCAR-8 cell line (Fig. 1), suggesting that acquisition of multidrug drug resistance does not affect *ASNS* expression. Significantly, siASNS transfection yielded >700-fold potentiation of L-ASP activity in OVCAR-8/ADR cells (Fig. 3C), showing that the causal link between ASNS expression and L-ASP activity survives the development of classical multidrug resistance. That potentiation was reproducible; a second, independent experiment yielded 840- and 880-fold potentiation with siASNS.1 and siASNS.2, respectively (data not shown).

ASNS Antibody Stains Ovarian Cell Lines Differentially in Accord with Microarray and Western Blot Data

Immunohistochemical staining using a rabbit polyclonal antibody against ASNS showed differential staining of the ovarian cell lines (Fig. 4). The order of staining intensities was OVCAR-4 > OVCAR-3 > OVCAR-5 > OVCAR-8, consistent with the relative expression levels determined for *ASNS* mRNA by microarray (Fig. 1) and by branched-DNA assay (Fig. 2A) and for ASNS protein by Western blot (Fig. 2B). In each culture, all cells stained to about the same intensity.

Tissue Array Screening for Clinical Cancers Low in ASNS

To begin assessment of the potential of ASNS as a biomarker in clinical tumors, we examined ASNS expression in a variety of cancer types using tissue microarrays from the NCI TARP (20). For qualitative analysis, each tumor specimen was scored as 0, 1+, 2+, or 3+ depending

on the intensity (negative, weak, moderate, strong) and pervasiveness of staining. For heuristic purposes, 0 and 1+ were considered ''low.'' ASNS levels were scored as low in 15% (8 of 54) of ovarian cancers, 2% (1 of 46) of prostate cancers, 17% (6 of 35) of breast cancers, 19% (12 of 63) of colon cancers, 23% (18 of 77) of lung cancers, 55% (12 of 22) of lymphomas, and 64% (7 of 11) of head and neck tumors. We also did preliminary studies with ovarian cancer tissue arrays from Cybrdi (60 primary ovarian tumors) and US Biomax (172 primary ovarian tumors; Fig. 5). A range of staining intensity was observed (Fig. 5A), and, importantly, that intensity was essentially uniform across all tumor cells in a given core (Fig. 5B and C), providing further rationale for clinical use of L-ASP and use of the antibody in evaluation of ASNS as a biomarker.

Discussion

Recent advances in bioinformatics and pharmacogenomics toward the goal of personalized medicine are helping to identify new uses for clinically approved drugs (21–27). In that context, we report here the investigation of a pharmacogenomic/pharmacoproteomic correlation between *ASNS* expression and L-ASP activity in ovarian cancer cell lines of the NCI-60 human cancer cell line panel. Studies using four different microarray platforms all showed negative Pearson correlations between *ASNS* expression and L-ASP activity (Fig. 1). The correlation coefficients ranged from −0.85 to −0.90 for the four platforms (the top 0.3 to 2.4 percentile for negative correlation when compared with all of the gene/L-ASP correlations across the genome). BAC arrays then showed an even stronger negative correlation of L-ASP activity with 7q DNA copy number (Fig. 1, *aCGH*; −0.98; 0.4 percentile), providing a plausible mechanism to explain the correlation with expression. We do not know why the correlation seemed to be strongest at the DNA copy level; perhaps the CGH technology was more accurate or perhaps it was chance. Regardless of the answer, the correlation was statistically significant on all platforms. Because the ASNS/L-ASP pair in ovarian cancer was already the focus of attention based on prior literature and our prior results, no multiple comparison correction was necessary. The high negative values suggest ASNS levels as the principal determinant of L-ASP activity in the cells.

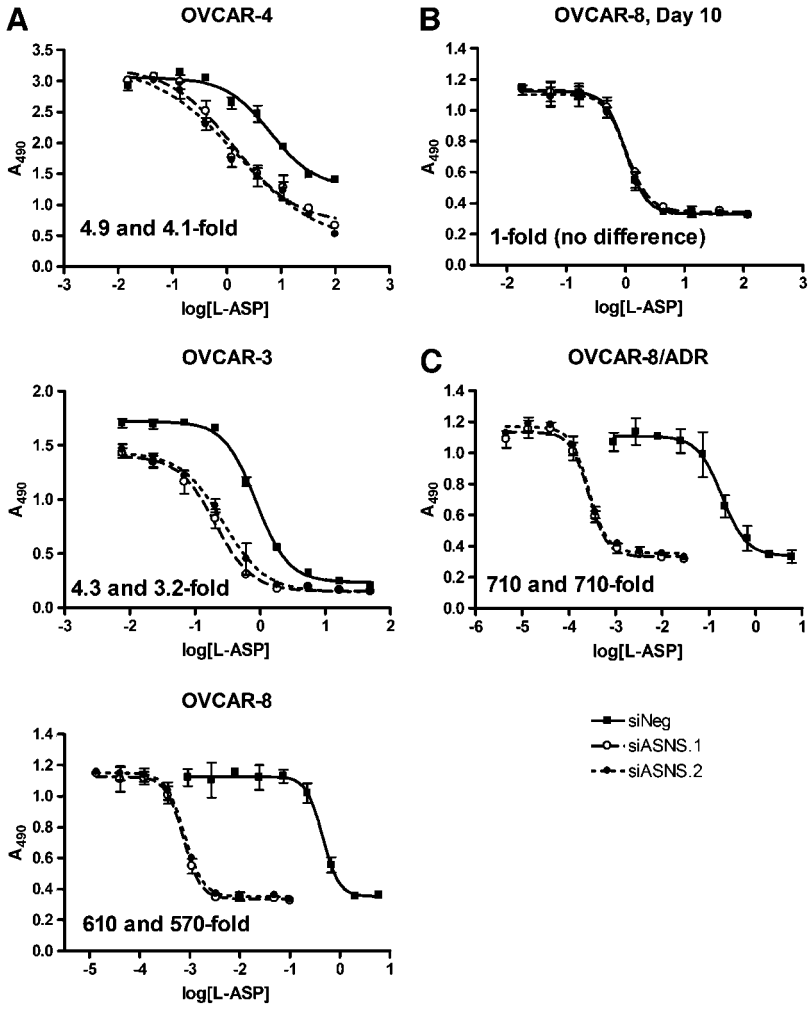

Figure 3. Effect of RNAi against *ASNS* on L-ASP activity. **A,** ovarian cell lines transfected with siRNA, treated with L-ASP starting 48 h later, and assayed with MTS 48 to 72 h thereafter. **B,** OVCAR-8 cells exposed to L-ASP starting on day 8 after the transient siRNA transfection (i.e., when ASNS levels had returned essentially to baseline) and assayed with MTS on day 10. **C,** OVCAR-8/ADR cells (selected for resistance to Adriamycin) treated as described in (**A**). Representative single experiments.

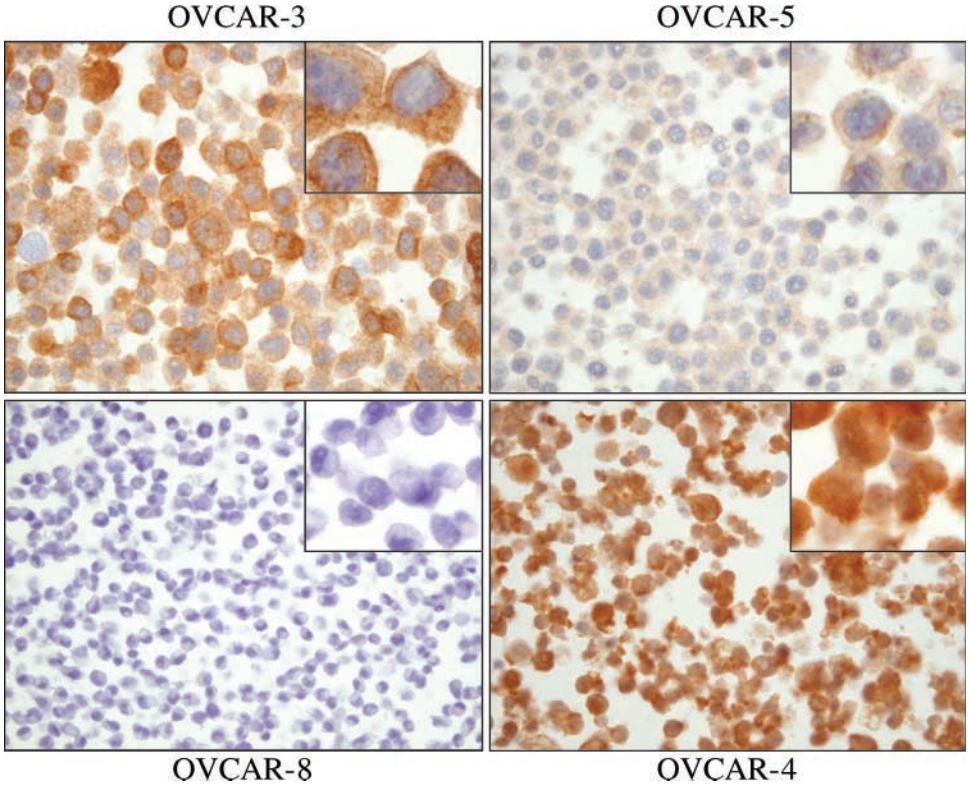

Figure 4. ASNS levels assessed by immunohistochemical staining of ovarian cell lines with a rabbit polyclonal antibody. The images are consistent with the findings in Fig. 1 from multiple microarray platforms; OVCAR-3 and OVCAR-4 express relatively high levels of ASNS, whereas OVCAR-5 expresses less, and OVCAR-8 expresses the least (40×/0.75 and 100×/1.30 objectives).

We next used RNAi against *ASNS* to assess whether the expression-activity correlation is causal or epiphenomenal; a causal relationship would provide a more direct association and, hence, a stronger rationale for clinical testing of L-ASP in a low-ASNS subset of ovarian cancer patients. Transfection of synthetic siRNAs targeted to *ASNS* yielded substantial (~80%) silencing of both mRNA and protein expression (Fig. 2), and that silencing resulted in potentiation of L-ASP activity in all three ovarian cell lines tested (Fig. 3). Those findings showed that the ASNS/L-ASP relationship is causal.

The striking >500-fold potentiation of L-ASP activity observed on 5-fold ASNS knockdown in the low-ASNS OVCAR-8 cell line and its OVCAR-8/ADR counterpart (Fig. 3A and C) may actually be a result of ''resistance'' rather than ''potentiation.'' Previous reports have shown that ASNS expression can be induced rapidly in leukemic and nonleukemic cell lines by L-ASP treatment (28, 29) and that a mere 7-fold induction of *ASNS* mRNA can yield a >1,000-fold increase in resistance to L-ASP (29). Our data are consistent with those observations. The MTS curves for siASNS-transfected cells probably reflect L-ASP activity with ASNS kept low, whereas the curves for siNeg-transfected cells (or cells not siRNA-transfected at all) were probably shifted to the right (i.e., toward resistance) because of rapid ASNS up-regulation during the 48-hour period of exposure to L-ASP. Regardless of mechanism, the potentiation we observed with siASNS for all three cell lines shows a causal link between L-ASP activity and ASNS expression.

We next asked whether L-ASP would be active in multidrug-resistant cancer cells, because classical multidrug resistance precludes therapy with a variety of standard agents (e.g., paclitaxel, a first-line drug for treatment of clinical ovarian cancer). As might have been expected in that context, the NCI-60 screen data showed OVCAR-8/ADR, a multidrug-resistant line selected from OVCAR-8 by exposure to Adriamycin (doxorubicin), to be 32-fold less sensitive than the parental line to paclitaxel. In contrast, OVCAR-8/ADR showed approximately the same *ASNS* expression (Fig. 1) and L-ASP sensitivity (Fig. 3) as did the parental OVCAR-8, indicating that *ASNS* had not been up-regulated as part of the multidrug resistance phenotype. We then found that siASNS transfection led to L-ASP potentiation at least as great (>700-fold), confirming that the causal link between ASNS expression and L-ASP activity was still present after development of multidrug resistance.

Because ASNS catalyzes asparagine synthesis and L-ASP catalyzes the breakdown of asparagine, why did analysis of the NCI-60 data not reveal a strong inverse relationship between *ASNS* expression and L-ASP activity in cell types other than leukemic and ovarian? A likely explanation is that additional molecular species (or processes) affect L-ASP activity but are relatively unimportant in leukemic and ovarian cell lines. Those species or processes could explain why some cell lines with high ASNS levels have been reported to be sensitive to L-ASP, and some with low ASNS levels have been reported to be resistant (30). For example, because L-ASP can be toxic via glutamine

depletion (31–35), genes involved in glutamine-related pathways may play roles in the response to L-ASP. Despite the probable involvement of such molecular species in L-ASP activity, pharmacogenomic analysis of the NCI-60 data enabled us to identify cell types (i.e., leukemic and ovarian) for which ASNS expression seems to be a strong univariate predictor of L-ASP activity.

The potential value of ASNS as a biomarker is further suggested circumstantially by its causal relationship with L-ASP activity in the presence of previously established predictors of unfavorable treatment outcome. One such predictor is p53 mutation status; tumors with p53 mutations tend to be more chemoresistant than their wild-type counterparts (36–38). OVCAR-4 contains wild-type p53, whereas OVCAR-3 and OVCAR-8 contain two different p53 mutations (9b, 39, 40). It was promising to find that those p53 mutations did not confer resistance to L-ASP on silencing of ASNS. Second, *HER2* expression, which is associated with increased metastatic potential and decreased survival (41, 42), is 7-fold higher in OVCAR-4 than in OVCAR-8;[9] nonetheless, the causal link between ASNS expression and L-ASP activity was present in both lines. Third, epidermal growth factor receptor expression, which is also associated with poor prognosis (43, 44), is high in all three ovarian lines tested,[9] yet the relationship between ASNS and L-ASP was demonstrable in each. Fourth, CD10 negativity has been associated with resistance to L-ASP in leukemia cells (45), yet all three ovarian lines, which are CD10 negative, exhibited L-ASP potentiation on ASNS silencing. Fifth, a recent study in primary ovarian cancer cells identified genes differentially expressed in carboplatin-sensitive and carboplatin-resistant cells. ASNS was not among those genes (46), suggesting that the link between ASNS expression and L-ASP activity would survive the development of resistance to cisplatin and carboplatin, first-line agents for treatment of ovarian cancer. Sixth, a similar study in ovarian cell lines indicated that ASNS is not among the 22 genes on chromosomal arm 7q that are up-regulated in development of resistance to taxanes (47). All of those circumstantial observations, together with our demonstration that the causal relationship between ASNS expression and L-ASP activity survives the development of classical multidrug resistance in OVCAR-8/ADR (Fig. 3C), provide rationale for clinical testing of L-ASP in ovarian cancer patients whose tumors express low ASNS, even if other markers associated with resistance to chemotherapy are present. Any experimental results in cell lines must, of course, be tested clinically before their implications for treatment of human tumors are clear. Unfortunately, mice, unlike humans, express endogenous L-ASP (at high levels; ref. 48), so they are questionable as models for assessment of ASNS as a biomarker for asparagine depletion therapy.

We next asked whether a subset of clinical ovarian cancers would show low ASNS expression. To address that

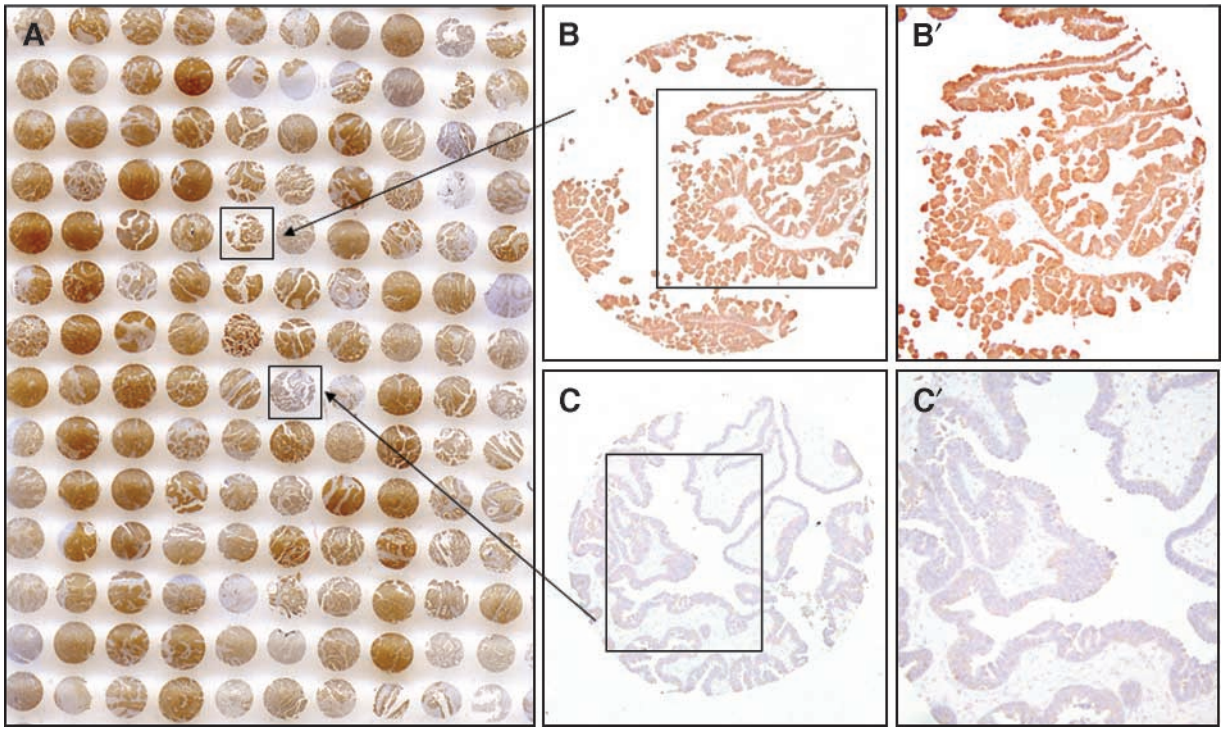

Figure 5. ASNS levels in an ovarian cancer tissue microarray as detected immunohistochemically with a rabbit polyclonal antibody. **A,** overview scan of US Biomax array (excluding cores at the margins of the array because of edge-effects in the staining). The column of six cores at bottom left consists of ''control'' squamous cell tumors. **B** and **C,** magnified (×10/0.3 objective) images of ASNS-positive and ASNS-negative cores, respectively. **B′** and **C′,** higher-magnification (40×/0.75 objective) images of the respective cores.

question, we first tested our rabbit polyclonal anti-ASNS antibody against ovarian cell line pellets and found that it stained the lines differentially (Fig. 4), in accord with the quantitative results from our four microarray data sets (Fig. 1) and Western blots (Fig. 2B). We then used the same antibody to stain microarrays of tumors taken directly from patients (Fig. 5) and to estimate the percentages of low-ASNS specimens. Two points should be noted in interpreting those percentages: (*i*) intensity of staining for any particular tumor core may be influenced by the way in which the core was fixed and embedded; (*ii*) the cutoff at 1+ staining is arbitrary; we do not yet know how the score relates to functional differences in response to L-ASP. Therefore, the principal information to be gleaned from the arrays comes from comparison of tumor types. Bearing that in mind, head and neck tumors as well as lymphomas clearly showed the greatest percentages of low expressers (64% and 55%, respectively). The head and neck finding may be interesting in its own right, although it is not central to the focus of this study on ovarian cancer cells; until cetuximab this year, the last chemotherapeutic agent to be approved for treatment of head and neck cancer was methotrexate in the 1950s. L-ASP therapy for head and neck tumors should therefore be considered, and we plan to use *ASNS*-targeted siRNA to test the causality of the ASNS/L-ASP relationship in head and neck cell lines. At the other end of the spectrum were the prostate cancers (2%), and ovarian (15%) was near the middle. If, hypothetically, 15% of ovarian cancers were responsive to L-ASP on the basis of low ASNS, one would not have enough statistical power to identify the responders in a clinical trial of moderate size unless ASNS were used as a biomarker for patient selection or in analysis of the responses.

Clear cell ovarian cancers have been reported to express lower ASNS levels than do endometrioid, mucinous, serous, or mixed ovarian cancers ($P = 0.001$; ref. 49). That observation is interesting because clear cell cancers usually have the worst prognosis. In our immunostaining, the two clear cell samples on Cybrdi arrays were scored as low expressers. The US Biomax array did not include any clear cell samples. Another study showed lower ASNS expression in ovarian adenocarcinoma samples than in normal ovary ($P < 0.007$; ref. 50).

In conclusion, we have shown a causal relationship between L-ASP activity and the expression of both *ASNS* transcript and ASNS protein in ovarian cancer cell lines. Of course, nothing is entirely simple and straightforward in biology; as indicated in an excellent recent review (51), other molecular players and processes can clearly be influential. However, if the relationship we have identified in cell lines carries over into clinical ovarian cancer (as it does in the case of lymphoid malignancies), our results suggest that ovarian tumors with moderate to low levels of ASNS may be sensitive to depletion of extracellular asparagine. The apparent mechanism of action is particularly interesting because it differs from those of the standard cytotoxic drug classes and because it does not require L-ASP to escape from the bloodstream or penetrate tumor substance. Penetration of the tumor is a major problem with many other protein (and small molecule) therapeutics (52). Asparagine depletion could, in principle, be achieved with L-ASP, siASNS, and/or a low molecular weight inhibitor of ASNS (e.g., one of the *N*-acylsulfonamide or sulfoxamine derivatives developed for that purpose; ref. 53). For now, our findings provide rationale for clinical testing of L-ASP against low-ASNS subsets of ovarian cancers (and perhaps other cancer types), with ASNS as a causally linked biomarker. Toward that end, we have opened a phase I clinical trial at three academic institutions to test the safety of polyethylene glycolated L-ASP (in combination with gemcitabine) in patients with solid tumors and non-Hodgkin's lymphoma, with retrospective assessment of ASNS as a biomarker.

Acknowledgments

We thank Tamara Jones and Cheryl Thomas (Gene Silencing Section, Center for Cancer Research, NCI) for technical assistance; the staff of the NCI Developmental Therapeutics Program for their work on the NCI-60 screening panel; and Eric Kaldjian, Jeffey Cossman, and Douglas Dolginow at GeneLogic, Inc. for the fine collaboration that produced our HG-U95 and HG-U133 transcript expression values for ASNS. The RNAi reagents used in this study were supplied to NCI by Qiagen as part of a Collaborative Research Agreement; we thank Eric Lader and Qiagen for design and synthesis of the *ASNS* siRNAs.

References

1. Kiriyama Y, Kubota M, Takimoto T, et al. Biochemical characterization of U937 cells resistant to L-asparaginase: the role of asparagine synthetase. Leukemia 1989;3:294–7.

2. Scherf U, Ross DT, Waltham M, et al. A gene expression database for the molecular pharmacology of cancer. Nat Genet 2000;24:236–44.

3. Stams WA, den Boer ML, Beverloo HB, et al. Sensitivity to L-asparaginase is not associated with expression levels of asparagine synthetase in t(12;21)+ pediatric ALL. Blood 2003;101:2743–7.

4. Paull KD, Shoemaker RH, Hodes L, et al. Display and analysis of patterns of differential activity of drugs against human tumor cell lines: development of mean graph and COMPARE algorithm. J Natl Cancer Inst 1989;81:1088–92.

5. Monks A, Scudiero D, Skehan P, et al. Feasibility of a high-flux anticancer drug screen using a diverse panel of cultured human tumor cell lines. J Natl Cancer Inst 1991;83:757–66.

6. Stinson SF, Alley MC, Kopp WC, et al. Morphological and immunocytochemical characteristics of human tumor cell lines for use in a disease-oriented anticancer drug screen. Anticancer Res 1992;12:1035–53.

7. Boyd MR. Status of the NCI preclinical antitumor drug discovery screen. In: DeVita VT, Hellman S, Rosenberg SA, editors. Cancer: principles and practice of oncology update. Philadelphia: J.B. Lippicott; 1989. p. 1–12.

8. Weinstein JN, Kohn KW, Grever MR, et al. Neural computing in cancer drug development: predicting mechanism of action. Science 1992;258:447–51.

9. Weinstein JN, Myers TG, O'Connor PM, et al. An information-intensive approach to the molecular pharmacology of cancer. Science 1997;275:343–9.

9a. Weinstein JN. Spotlight on molecular profiling: "integromic" analysis of the NCI-60 cancer cell lines. Mol Cancer Ther, this issue.

9b. Ikediobi ON, Davies H, Bignell G, et al. Mutation analysis of 24 known cancer genes in the NCI-60 cell line set. Mol Cancer Ther, this issue.

10. Bussey KJ, Chin K, Lababidi S, et al. Integrating data on DNA copy number with gene expression levels and drug sensitivities in the NCI-60 cell line panel. Mol Cancer Ther 2006;5:853–67.

11. Ross DT, Scherf U, Eisen MB, et al. Systematic variation in gene expression patterns in human cancer cell lines. Nat Genet 2000;24:227–35.

12. Staunton JE, Slonim DK, Coller HA, et al. Chemosensitivity prediction by transcriptional profiling. Proc Natl Acad Sci U S A 2001;98:10787–92.

13. Hewitt SM. Design, construction, and use of tissue microarrays. Methods Mol Biol 2004;264:61–72.

14. Nishizuka S, Charboneau L, Young L, et al. Proteomic profiling of the NCI-60 cancer cell lines using new high-density reverse-phase lysate microarrays. Proc Natl Acad Sci U S A 2003;100:14229–34.

15. Anderson L, Seilhamer J. A comparison of selected mRNA and protein abundances in human liver. Electrophoresis 1997;18:533–7.

16. Alley MC, Scudiero DA, Monks A, et al. Feasibility of drug screening with panels of human tumor cell lines using a microculture tetrazolium assay. Cancer Res 1988;48:589–601.

17. Batist G, Tulpule A, Sinha BK, Katki AG, Myers CE, Cowan KH. Overexpression of a novel anionic glutathione transferase in multidrug-resistant human breast cancer cells. J Biol Chem 1986;261:15544–9.

18. Cowan KH, Batist G, Tulpule A, Sinha BK, Myers CE. Similar biochemical changes associated with multidrug resistance in human breast cancer cells and carcinogen-induced resistance to xenobiotics in rats. Proc Natl Acad Sci U S A 1986;83:9328–32.

19. Roschke AV, Tonon G, Gehlhaus KS, et al. Karyotypic complexity of the NCI-60 drug-screening panel. Cancer Res 2003;63:8634–47.

20. Kononen J, Bubendorf L, Kallioniemi A, et al. Tissue microarrays for high-throughput molecular profiling of tumor specimens. Nat Med 1998;4:844–7.

21. Alizadeh AA, Eisen MB, Davis RE, et al. Distinct types of diffuse large B-cell lymphoma identified by gene expression profiling. Nature 2000;403:503–11.

22. Stoughton RB, Friend SH. How molecular profiling could revolutionize drug discovery. Nat Rev Drug Discov 2005;4:345–50.

23. Evans WE, Relling MV. Pharmacogenomics: translating functional genomics into rational therapeutics. Science 1999;286:487–91.

24. Ransohoff DF. Rules of evidence for cancer molecular-marker discovery and validation. Nat Rev Cancer 2004;4:309–14.

25. Ludwig JA, Weinstein JN. Biomarkers in cancer staging, prognosis and treatment selection. Nat Rev Cancer 2005;5:845–56.

26. Blower PE, Yang C, Fligner MA, et al. Pharmacogenomic analysis: correlating molecular substructure classes with microarray gene expression data. Pharmacogenomics J 2002;2:259–71.

27. Weinstein JN. Pharmacogenomics–teaching old drugs new tricks. N Engl J Med 2000;343:1408–9.

28. Aslanian AM, Fletcher BS, Kilberg MS. Asparagine synthetase expression alone is sufficient to induce l-asparaginase resistance in MOLT-4 human leukaemia cells. Biochem J 2001;357:321–8.

29. Hutson RG, Kitoh T, Moraga Amador DA, Cosic S, Schuster SM, Kilberg MS. Amino acid control of asparagine synthetase: relation to asparaginase resistance in human leukemia cells. Am J Physiol 1997;272:C1691–9.

30. Ando M, Sugimoto K, Kitoh T, et al. Selective apoptosis of natural killer-cell tumours by l-asparaginase. Br J Haematol 2005;130:860–8.

31. Kafkewitz D, Bendich A. Enzyme-induced asparagine and glutamine depletion and immune system function. Am J Clin Nutr 1983;37:1025–30.

32. Villa P, Corada M, Bartosek I. L-asparaginase effects on inhibition of protein synthesis and lowering of the glutamine content in cultured rat hepatocytes. Toxicol Lett 1986;32:235–41.

33. Kitoh T, Asai S, Akiyama Y, Kubota M, Mikawa H. The inhibition of lymphocyte blastogenesis by asparaginase: critical role of glutamine in both T and B lymphocyte transformation. Acta Paediatr Jpn 1992;34:579–83.

34. Fumarola C, Zerbini A, Guidotti GG. Glutamine deprivation-mediated cell shrinkage induces ligand-independent CD95 receptor signaling and apoptosis. Cell Death Differ 2001;8:1004–13.

35. Reinert RB, Oberle LM, Wek SA, et al. Role of glutamine depletion in directing tissue-specific nutrient stress responses to L-asparaginase. J Biol Chem 2006;281:31222–33.

36. Bergh J, Norberg T, Sjogren S, Lindgren A, Holmberg L. Complete sequencing of the p53 gene provides prognostic information in breast cancer patients, particularly in relation to adjuvant systemic therapy and radiotherapy. Nat Med 1995;1:1029–34.

37. Cadwell C, Zambetti GP. The effects of wild-type p53 tumor suppressor activity and mutant p53 gain-of-function on cell growth. Gene 2001;277:15–30.

38. Campling BG, el-Deiry WS. Clinical implications of p53 mutations in lung cancer. Methods Mol Med 2003;75:53–77.

39. O'Connor PM, Jackman J, Bae I, et al. Characterization of the p53 tumor suppressor pathway in cell lines of the National Cancer Institute anticancer drug screen and correlations with the growth-inhibitory potency of 123 anticancer agents. Cancer Res 1997;57:4285–300.

40. Olivier M, Eeles R, Hollstein M, Khan MA, Harris CC, Hainaut P. The IARC TP53 database: new online mutation analysis and recommendations to users. Hum Mutat 2002;19:607–14.

41. Menard S, Tagliabue E, Campiglio M, Pupa SM. Role of HER2 gene overexpression in breast carcinoma. J Cell Physiol 2000;182:150–62.

42. Slamon DJ, Clark GM, Wong SG, Levin WJ, Ullrich A, McGuire WL. Human breast cancer: correlation of relapse and survival with amplification of the HER-2/neu oncogene. Science 1987;235:177–82.

43. Maurizi M, Scambia G, Benedetti Panici P, et al. EGF receptor expression in primary laryngeal cancer: correlation with clinico-pathological features and prognostic significance. Int J Cancer 1992;52:862–6.

44. Buerger H, Gebhardt F, Schmidt H, et al. Length and loss of heterozygosity of an intron 1 polymorphic sequence of egfr is related to cytogenetic alterations and epithelial growth factor receptor expression. Cancer Res 2000;60:854–7.

45. Ramakers-van Woerden NL, Beverloo HB, Veerman AJ, et al. *In vitro* drug-resistance profile in infant acute lymphoblastic leukemia in relation to age, MLL rearrangements and immunophenotype. Leukemia 2004;18:521–9.

46. Peters D, Freund J, Ochs RL. Genome-wide transcriptional analysis of carboplatin response in chemosensitive and chemoresistant ovarian cancer cells. Mol Cancer Ther 2005;4:1605–16.

47. Wang YC, Juric D, Francisco B, et al. Regional activation of chromosomal arm 7q with and without gene amplification in taxane-selected human ovarian cancer cell lines. Genes Chromosomes Cancer 2006;45:365–74.

48. Milman HA, Cooney DA. The distribution of L-asparagine synthetase in the principal organs of several mammalian and avian species. Biochem J 1974;142:27–35.

49. Schwartz DR, Kardia SL, Shedden KA, et al. Gene expression in ovarian cancer reflects both morphology and biological behavior, distinguishing clear cell from other poor-prognosis ovarian carcinomas. Cancer Res 2002;62:4722–9.

50. Lancaster JM, Dressman HK, Whitaker RS, et al. Gene expression patterns that characterize advanced stage serous ovarian cancers. J Soc Gynecol Investig 2004;11:51–9.

51. Richards NG, Kilberg MS. Asparagine synthetase chemotherapy. Annu Rev Biochem 2006;75:629–54.

52. Saga T, Neumann RD, Heya T, et al. Targeting cancer micrometastases with monoclonal antibodies: a binding-site barrier. Proc Natl Acad Sci U S A 1995;92:8999–9003.

53. Koroniak L, Ciustea M, Gutierrez JA, Richards NG. Synthesis and characterization of an N-acylsulfonamide inhibitor of human asparagine synthetase. Org Lett 2003;5:2033–6.